Langmuir

Article

pubs.acs.org/Langmuir

Synergism between Airborne Singlet Oxygen and a Trisubstituted Olefin Sulfonate for the Inactivation of Bacteria

Rajib Choudhury and Alexander Greer*

Department of Chemistry and Graduate Center, City University of New York, Brooklyn College, Brooklyn, New York 11210, United States

Supporting Information

ABSTRACT: The reactivity of a trisubstituted alkene surfactant (8-methylnon-7-ene-1 sulfonate, **1**) to airborne singlet oxygen in a solution containing *E. coli* was examined. Surfactant **1** was prepared by a Strecker-type reaction of 9-bromo-2-methylnon-2-ene with sodium sulfite. Submicellar concentrations of **1** were used that reacted with singlet oxygen by an "ene" reaction to yield two hydroperoxides (7-hydroperoxy-8-methylnon-8-ene-1 sulfonate and (*E*)-8-hydroperoxy-8-methylnon-6-ene-1 sulfonate) in a 4:1 ratio. Exchanging the H_2O solution for D_2O where the lifetime of solution-phase singlet oxygen increases by 20-fold led to an ∼2-fold increase in the yield of hydroperoxides pointing to surface activity of singlet oxygen with the surfactant in a partially solvated state. In this airborne singlet oxygen reaction, *E. coli* inactivation was monitored in the presence and absence of **1** and by a LIVE/DEAD cell permeabilization assay. It was shown that the surfactant has low dark toxicity with respect to the bacteria, but in the presence of airborne singlet oxygen, it produces a synergistic enhancement of the bacterial inactivation. How the ene-derived surfactant hydroperoxides can provoke $^1O_2$ toxicity and be of general utility is discussed.

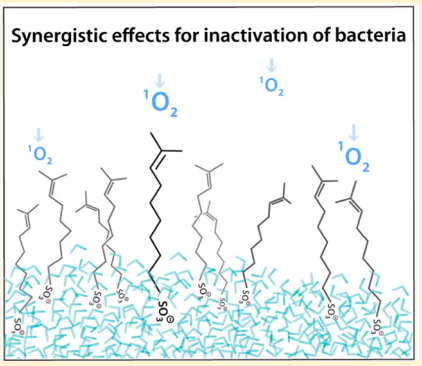

INTRODUCTION

Although singlet oxygen [$^1O_2$ ($^1\Delta_g$)] is an effective toxin for inactivating bacteria,[1,2] methods to generate it suffer from photosensitizer problems including solubilization,[3−5] degradation, and bleaching.[6] Turbid solutions[7,8] can also present problem because light can be blocked from reaching the sensitizer. Because of these issues, there is a need to develop methods for killing bacteria without the physical contact of photosensitizer with the solution. Airborne $^1O_2$ offers some promise in this regard.[9−13]

Figure 1 shows the three-phase apparatus that we used in this study for the delivery of $^1O_2$ to the air/water interface of a bacterial solution. By virtue of how the apparatus works, the solution is devoid of any photosensitizers, where gas-phase singlet oxygen diffuses to the solution surface. By analogy, Majima et al.[9,10] carried out experiments using a sensitizing TiO_2 surface and a terrylenediimide oxygen acceptor adsorbed on another surface that was separated by over 1 mm, indicating the formation of a diffusible $^1O_2$ species (similar to the Kautsky three-phase test of 80 years ago).[14,15]

That the apparatus in Figure 1 leads to $^1O_2$ at the air/water interface for *E. coli* inactivation is not surprising because its design is similar to that of an apparatus invented by Midden.[13] What is new and better (we regard our innovation as an offshoot of the Midden and Majima systems) is the unique function of surfactant **1** in *E. coli* inactivation by airborne $^1O_2$.

Our hypothesis was that a $^1O_2$-active surfactant (**1**) would synergistically enhance bacterial inactivation. Synergy has been found in other branches of singlet oxygen research. It has been found in the photodynamic inactivation of bacteria with biofilm dispersions of a 2-aminoimidazole-triazole conjugate,[16] in photodynamic therapy (PDT) with drug additives such as carboplatin,[17] and with the simultaneous reaction of nitric oxide[18] or $SO_3^{\bullet-}$,[19] among other $^1O_2$ topics. Similar to surfactant **1**, there was a report on a 2,5-disubstituted furan surfactant with a cationic tetraalkylammonium headgroup that was oxidized by $^1O_2$ to an endoperoxide in a liposome study,[20] but the reaction was not examined for antibacterial activity.

Here we show that an $^1O_2$-active surfactant can synergistically enhance microbe inactivation from airborne $^1O_2$ through hydroperoxide formation. Our work serves as a starting point where in-situ-generated surfactant hydroperoxides function as secondary toxins to pure $^1O_2$ for enhanced bactericidal action. Following the Experimental Section, our results will be presented in four parts: first, the rationale for the selection of surfactant **1**; second, measured surfactant photoperoxide formation via airborne $^1O_2$; third, measured *E. coli* killing by $^1O_2$ with and without surfactant **1**; and fourth, measured *E. coli* killing by $^1O_2$, followed by the addition of hydroperoxides **2** and **3** in the dark.

EXPERIMENTAL SECTION

Reagents and Instrumentation. Porous Vycor glass (Corning 7930) was purchased from Advanced Glass and Ceramics (Holden,

Received: November 27, 2013
Revised: January 26, 2014
Published: March 10, 2014

   dx.doi.org/10.1021/la404564k | Langmuir 2014, 30, 3599−3605

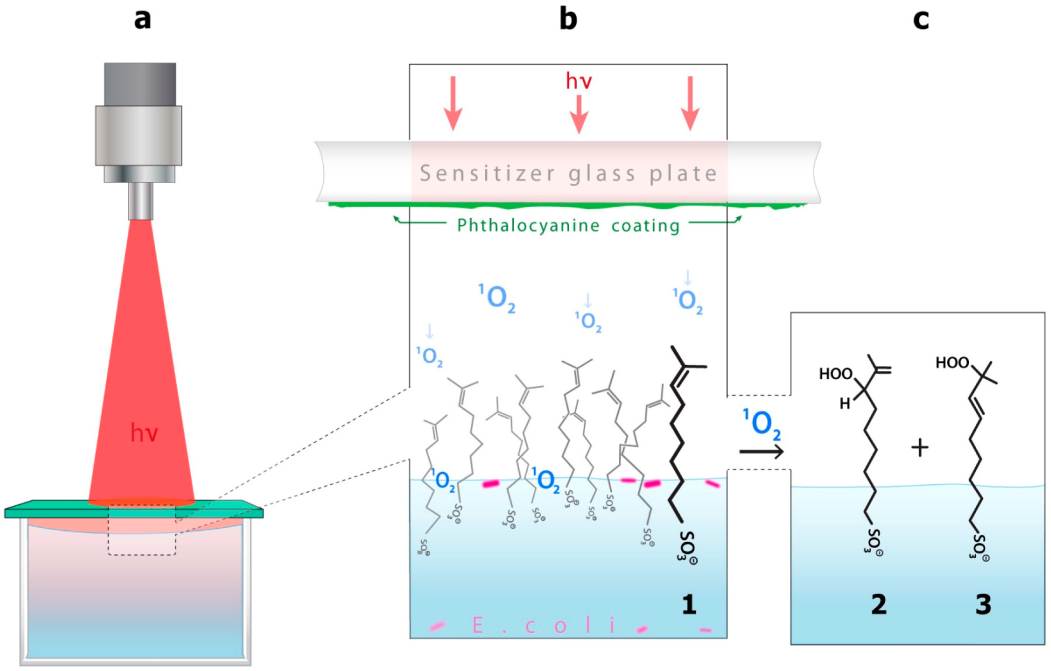

Figure 1. (a) Red 669 nm light is directed in from above to a glass plate whose bottom side is coated with aluminum(III) phthalocyanine chloride tetrasulfonic acid (Pc). (b) O_2 is sensitized by excited Pc sites on the plate where $^1O_2$ traverses a ~0.4−1.5 mm distance to reach the *E. coli* solution of 0.1 mM surfactant **1**, where (c) hydroperoxides **2** and **3** are produced.

MA). Silicon phthalocyanine dichloride, aluminum(III) phthalocyanine chloride tetrasulfonic acid, 9-bromo-2-methylnon-2-ene, sodium sulfite, triphenyl phosphine (PPh_3), benzoic acid, dimethylsulfone, DMF, CH_2Cl_2, ethanol, D_2O, and DMSO-d_6 were purchased from commercial suppliers and were used as received. Dichloromethane was distilled over phosphorus pentoxide prior to use. Deionized water was purified with a U.S. Filter Corporation deionization system (Vineland, NJ). Nuclear magnetic resonance (NMR) data were recorded on a Bruker Avance 400 spectrometer operating at 400 MHz for ^1H NMR and at 100.6 MHz for ^{13}C NMR. UV−vis data were collected on a Hitachi UV−vis U-2001 instrument. FAB-mass spectrometry data were collected on a JEOL JMS-HX110 spectrometer using a *m*-nitrobenzyl alcohol matrix, a 10 kV acceleration voltage, and a Xe beam FAB gun (6 kV) on the MS-1 ion source. Infrared spectra were recorded on a Nicolet iS10 FT-IR spectrometer. Solution temperatures were measured with a digital pyrometer (Thermo Scientific). An Olympus FluoView FV10i confocal fluorescence microscope was used to analyze stained *E. coli* and assess membrane permeability following singlet oxygen exposure.

Sensitizing Glass Plate. Using a Pasteur pipet, 50 μL of methanol containing 8×10^{-4} M aluminum(III) phthalocyanine chloride tetrasulfonic acid (Pc) was deposited onto one side of PVG (disk shape 14.0 mm × 1.0 mm or square shape 2.25 cm^2 and 1.0−1.5 mm). Most of the methanol had evaporated after 12−24 h at 26 °C, at which point the sample was used. The result was PVG sensitizing glass loaded on one side with 1.1×10^{-5} mols of Pc/g of PVG with the penetration of the sensitizer into the glass core and edges.

Apparatus. A three-phase apparatus was constructed for airborne $^1O_2$ delivery to the air/water interface of a solution (Figures 2). The sensitizing glass plate was placed sensitizer face down, above a short quartz cuvette ($1.0 \times 1.0 \times 0.7$ cm^3) containing 0.60 mL of water (from a micropipet, precision ±0.005 mL) and illuminated perpendicularly from a 3.0 cm distance with 669 nm light (383 mW) from a diode laser (model 7404, Intense, North Brunswick, NJ). The light from the laser overlapped well[21] with the Pc absorption. The 669 nm light was passed through an FT-400-EMT optical fiber (Thorlabs, Newton NJ), which produced a Gaussian distribution of incident photons on the sensitizing glass plate (total dose ≈ 1700 J/cm^2). The diameter of the laser spot on the sensitizer glass plate was

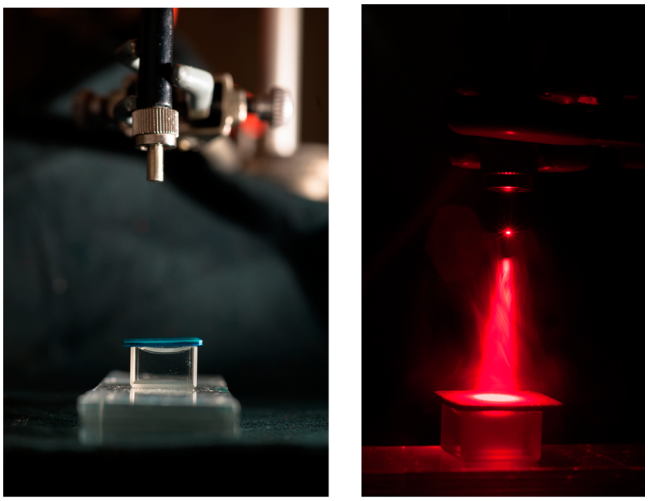

a b

Figure 2. Apparatus for generating airborne $^1O_2$ where it travels a short distance to a solution containing surfactant **1** and *E. coli*. (a) A sensitizer glass plate covers but does not contact the water solution in the quartz cuvette. (b) Red 669 nm light is directed in from above via an optical fiber connected to a diode laser. A piece of white paper was placed in front of the beam and moved downward to capture the approximate path of the beam contacting the sensitizer plate (Nikon digital camera settings: ISO 100, F20, and 1/50 s flash burst, 3 s total exposure).

0.95 cm (area = 0.71 cm^2). The sensitizer glass plate was not in contact with the water. The sensitizing glass plate sat atop the short cuvette above the water interface by 0.4 mm situated at the sides of the cuvette. Moving laterally from the cuvette side to the midpoint of the meniscus, the distance between the sensitizer plate and water was 1.5 mm. These distances were measured with a miniature ruler and a 10× magnifying glass with an uncertainty of ±0.04 mm. Water evaporation was negligible and did not measurably change the volume over the

dx.doi.org/10.1021/la404564k | *Langmuir* 2014, 30, 3599−3605

course of a 1 h experiment. The water temperature was increased by 3.5 ± 0.3 °C in 1 h, which slightly reduces the lifetime of singlet oxygen (by ~10 ns).[22] An analysis of the water samples after photolysis indicated that no Pc molecules had dislodged from the sensitizing glass nor had any relocated from the glass to the water.

Synthesis of Sodium 8-Methylnon-7-ene-1-sulfonate (1). Yield 38 mg (70%), purity >98%. A Strecker reaction between 9-bromo-2-methylnon-2-ene (0.05g, 0.22 mmol) and Na_2SO_3 (0.057g, 0.45 mmol) took place in 4 mL of refluxing DMF−water (1:1) under a nitrogen atmosphere in 12 h. After the mixture was cooled to room temperature, 2 mL of deionized H_2O and 2 mL of ethanol were added in succession. The filtrate was partitioned with CH_2Cl_2 (4 × 4 mL), and the CH_2Cl_2 fraction was discarded. The aqueous fraction was evaporated to dryness, leaving an off-white solid product that was recrystallized in ethanol−water (8:2). ^{1}H NMR (D_2O, 400 MHz): δ 5.1 (t, J = 14.8 Hz, 1H), 2.8 (t, J = 16 Hz, 2H), 1.93 (m, 2H), 1.68 (m, 2H), 1.64 (s, 1H), 1.56 (s, 1H), 1.36 (m, 2H), 1.29 (m, 4H). ^{13}C NMR (D_2O, 100.6 MHz): δ 133.2, 125.2, 51.1, 28.8, 27.9, 27.6, 27.1, 24.8, 24.0, 16.9. IR (neat) ν 2967, 2916, 2851, 1465, 1453, 1155 cm^{-1}. HRMS (FAB) m/z calcd for $[C_{10}H_{19}O_3SNa_2]^+$, 265.0849; found for $[C_{10}H_{19}O_3SNa_2]^+$, 265.0854. The solubility of surfactant **1** was 210 ± 20 g/L in deionized H_2O, and the critical micellar concentration (cmc) was 9.7 mM on the basis of an NMR titration method similar to that of Zhao and Fung[23] (Figure S9, Supporting Information).

Generation of Sodium 7-Hydroperoxy-8-methylnon-8-ene-1-sulfonate (2) and Sodium (*E*)-8-Hydroperoxy-8-methylnon-6-ene-1-sulfonate (3). Yield 1.4 mg (85% as a 4:1 mixture of **2**/**3**). After the reaction of **1** with $^1O_2$, water was removed under a stream of dry N_2. The residue was partitioned with chloroform (10 × 1 mL). The ratio of **2** and **3** was determined by ^{1}H NMR analysis of the 4.8 and 5.5 ppm protons and comparison with benzoic acid as an internal standard in DMSO-d_6. Hydroperoxides **2** and **3** were stable enough for characterization as a mixture, but they began to decompose after 1 to 2 days in D_2O at 26 °C. ^{1}H NMR (DMSO-d_6, 400 MHz): δ 11.2 (s, 1H), 10.8 (s, 1H), 5.5 (m, 2H), 4.8 (s, 2H), 4.1 (t, J = 14 Hz, 1H). ^{13}C NMR (DMSO-d_6, 100.6 MHz): δ 145.1, 135.2, 129.6, 113.3, 88.2, 80.8, 52.0, 32.3, 30.7, 29.4, 28.8, 25.5, 17.2. Control reactions showed that 669 nm irradiation of a piece of native PVG that had no Pc coating did not yield **2** and **3**. The addition of PPh_3 to the postreaction mixture[24] led to corresponding allylic alcohols that were also detected by NMR.

Microbial Studies. Bacterial strain CW 3747, a mutant of *E. coli* K_{12}, was purchased from the American Type Cells Collection (ATCC). Frozen stocks of *E. coli* (200 μL) were revived in 50 mL of Luria broth (LB) for 1 h and diluted to amounts ranging from 15 to 50 μg/mL as analyzed by UV−vis. Water samples were exposed to airborne $^1O_2$ via the apparatus for 10 min (or 20 or 30 min up to 60 min,) and 0.1 mL of the solution was poured onto agar plates. The samples were incubated at 37 °C for 24 h to determine the quantity of active colonies. *E. coli* was treated with surfactant **1** (1 mM) or hydroperoxides (0.01−0.2 mM 4:1 ratio of **2**/**3**) at different time intervals of 2 min to 1 h to determine the dark toxicity. Samples were assayed for cell viability by serial dilution in LB media and then plated in triplicate on LB with 1.5% agar. Control experiments were carried out in the absence of **1** in the dark. A LIVE/DEAD *Bac*Light bacterial viability kit (Molecular Probes, Eugene, OR) was used to stain the *E. coli* cells with SYTO-9 (diluted to 3.34 μM) and propidium iodide (diluted to 20 μM). Bacteria samples (50 μg/mL) were centrifuged for 5 min at 10 000*g*, and the pellets were suspended in deionized water by incubating each dye for 15 min at 37 °C, followed by analysis with fluorescence microscope.

Sources of Error. Error arises from three main sources: (1) compound weighing (~2%), (2) NMR peak integration (2 to 3%), and (3) bacterial colony counting, which was done manually at three different rotation angles per plate (reproducible to within ±2%).

RESULTS AND DISCUSSION

Selection of Surfactant Type and Conditions. An appealing hypothesis for the amplifying $^1O_2$ toxicity is the use of a surfactant that can readily form a hydroperoxide product. Thus, we selected terminally branched-chain olefin sulfonate **1** with an eye toward the ease of formation of allylic hydroperoxides. Trisubstituted olefins[25−27] are much more reactive with $^1O_2$ (~20−500-fold) than are di- and monosubstituted olefins.[28] For example, the chemical quenching rate constant (k_r) of $^1O_2$ with 2-methyl-2-pentene is reasonably high (6×10^5 M^{-1} s^{-1}).[29]

In the case of the detergent concentration, we selected a relatively low 1 mM concentration of **1** so the hydrophobic group would preferably point away from the surface. Our results show that the cmc of **1** ($C_{10}H_{19}SO_3^-$ Na^+) (9.7 mM at 26 °C) is lower than that of straight-chain $C_{10}H_{21}SO_3^-$ Na^+ (43 mM at 25 °C,[30] but similar to that of straight-chain $C_{12}H_{25}SO_3^-$ Na^+ (9.8[31] or 12 mM at 25 °C[30]). Although cmc's generally decrease for branched hydrophobic groups,[32] this mainly applies to internal rather than terminal unsaturated sites of olefin sulfonates. By running experiments below the micellar concentrations of **1**, the surfactant tends not to aggregate into environments away from the air/water interface.

Airborne Singlet Oxygen Attack on a Partially Solvated Surfactant. The apparatus brought airborne $^1O_2$ in from above onto the H_2O or D_2O solution for an ene reaction[33,34] with 1 mM detergent **1**. The two hydroperoxides that were formed (**2** and **3**) have a shift of the double bond relative to that of **1**, which is a fingerprint reaction[35] for singlet oxygen. We monitored the disappearance of **1** and the appearance of surfactant peroxides **2** and **3** (mass balance 91%), where **2** and **3** were stable enough for characterization as a mixture but began to decompose after 1 to 2 days at 26 °C.

Figure 3 shows that the airborne $^1O_2$ oxidation of **1** led to hydroperoxide products (**2** and **3**) at double the efficiency in

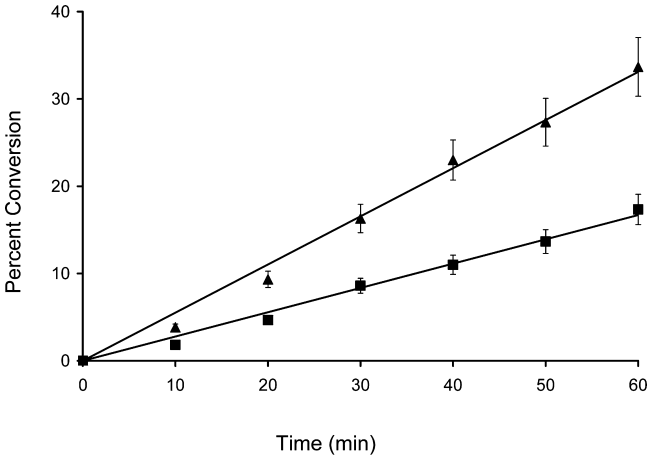

Figure 3. Reaction of airborne singlet oxygen with surfactant **1** at the air/water interface in D_2O (▲, R^2 = 0.9917) and in H_2O (■, R^2 = 0.9928). Ratio of slopes = 1.98.

D_2O as in H_2O (the yield was 18% in H_2O and 33% in D_2O). Because $^1O_2$ is not transferred deep into bulk water, it is not subject to the 20-fold τ_Δ increase in D_2O (69 μs at 20 °C) as in H_2O (3.5 μs at 20 °C).[22,36] Air moisture was found to introduce a small (~0.2%) amount of H_2O into the D_2O solution during the 1 h reaction period on the basis of the NMR integration of the HOD signal, but this was not an explanation of the modest product increase in D_2O. In D_2O, airborne $^1O_2$ reactions carried out with **1** above its cmc led a 2% yield of hydroperoxides **2** and **3** (far less than the 33% yield

dx.doi.org/10.1021/la404564k | Langmuir 2014, 30, 3599−3605

with **1** below its cmc) likely as a result of the micellar protection of the alkene site from incoming airborne $^1O_2$ at the air/water interface. Below the cmc, the results point to surface activity where airborne singlet oxygen attacks **1** in a partially solvated state.

Partially solvated **1** may relate to the observed stereoselectivity of hydroperoxides **2** and **3** because the ratio was 4:1 (Table 1). Hydrogen abstraction proceeds mostly from the methyl groups. Thus, the hexyl sulfonate chain in **1** is not acting as a bulky allylic group as could have been expected from curling conformations or else **3** rather than **2** would be the major product. It is known that $^1O_2$ geminal regioselectivity arises from bulky allylic groups on trisubstituted alkenes (Scheme 1)[37,38] and with vinyl silanes.[39] In the absence of sterics, the ene reaction of $^1O_2$ with trisubstituted alkenes, such as 2-methyl-2-pentene, usually yields the secondary and tertiary hydroperoxides in an ∼1:1 ratio with a slight favoring of the secondary hydroperoxide in polar solvents.[29] Some control of hydroperoxide product selectivity has been found for photooxidations if the alkene is contained in Nafion[40] and zeolites.[41,42] Secondary and tertiary hydroperoxides have been seen to decompose at different rates when encapsulated within zeolites,[43,44] but the obvious explanation that one of the hydroperoxides decomposes more rapidly prior to quantitation is not the case for **2** and **3**.

Table 1. Reaction of Methyl Nonene Sulfonate 1 with Airborne $^1O_2$ at or near the Air−Water Interface[a]

entry	medium of $^1O_2$	solution	% conversion after 1 h	product ratio **2**/**3**[b]
1	airborne	H_2O	18 ± 2	75:25 (±3)
2	airborne	D_2O	33 ± 3	79:21 (±2)

[a]Samples were illuminated at 669 nm. Airborne $^1O_2$ is generated and crosses an intervening gap to the H_2O or D_2O solution of **1** (1.0 mM). [b]Ratio of product calculated from the integration of the ^1H NMR 4.8 and 5.5 ppm signals. [c]Error bounds were obtained from three measurements.

Scheme 1

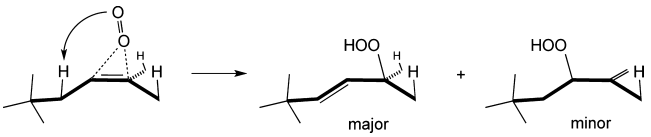

We tentatively attribute the 4:1 ratio of **2**/**3** to $^1O_2$ coming top down on the interface, where the methyl protons are surface "exposed" and more easily rotated than the methylene protons, with the latter being more wetted or anchored at the solution/air interface. In a transition-state model drawing (Scheme 2), we propose that the distal oxygen of the perepoxide transition structure preferably abstracts a methyl hydrogen prior to surface H bonding. Facile rotation[45,46] may be key, where the methylene allylic hydrogens of the hexyl sulfonate chain are more restricted to rotation and thus less conformationally accessible (higher barrier to rotation) than the methyl groups. We do not think that electronic repulsion[47] takes place between the distal perepoxide oxygen and the sulfonate anion to explain methyl rather than methylene H-abstraction regioselectivity.

We now turn our attention to the bacterial killing results.

Top-Down Approach to Bacterial Killing with Airborne $^1O_2$ and Surfactant 1. Here, we make a case that detergent **1** synergistically enhances the bactericidal action of incoming $^1O_2$. Table 2 shows that the apparatus produces airborne $^1O_2$ at levels toxic to bacteria (entries 1−3). Samples containing 50, 30, and 15 μg/mL *E. coli* were inactivated by 25, 38, and 41%, respectively, after 1 h. Table 3 (entry 5) shows that the inactivation of 50 μg/mL *E. coli* when followed in 10 min increments led to 27% killing after 1 h.

However, synergistic *E. coli* inactivation was seen when combining airborne $^1O_2$ and surfactant **1** (Table 2, entries 4−6). That is, the number of *E. coli* killed increased by 1.7- to 2-fold compared to $^1O_2$ treatment without **1**. The inactivation by **1** was 2.6% (entry 7) and by airborne $^1O_2$ was 25% (entry 1), which adds up to 27.6%, not the 50% seen with airborne $^1O_2$ in the presence of surfactant **1** (entry 4). The synergism was not restricted to the 50 μg/mL *E. coli* concentration but was also seen at 30 and 15 μg/mL.

Table 2 shows that the surfactant **1** toxicity in the dark is low. For example, for 50 μg/mL *E. coli*, 2.6% was killed by 1 mM **1**, and for 15 μg/mL *E. coli*, 7.3% was killed (entries 7−9). The addition of a 4:1 mixture of **2** (0.144 mM) and **3** (0.036 mM) (similar to the amount generated in situ in Figure 3) in the dark was also relatively nontoxic, and the mixture led to 5−8% *E. coli* inactivation (Table 2, entries 10−12). Entry 13 shows a control reaction of the *E. coli* viability of 1.5% in the dark without surfactant **1** or hydroperoxides **2** and **3**. The red light emitted from the device was also mostly nontoxic to *E. coli*, and the inactivation ranged from 3.7 to 8% for *E. coli* concentrations of 50 to 15 μg/mL (Table 2, entries 14−16). These observations point to low levels of 3−8% *E. coli* inactivation based on additives **1**−**3** in the dark or in red light alone. Next, we explored the effects of incubating hydroperoxides **2** and **3** with $^1O_2$-pretreated cells.

Scheme 2

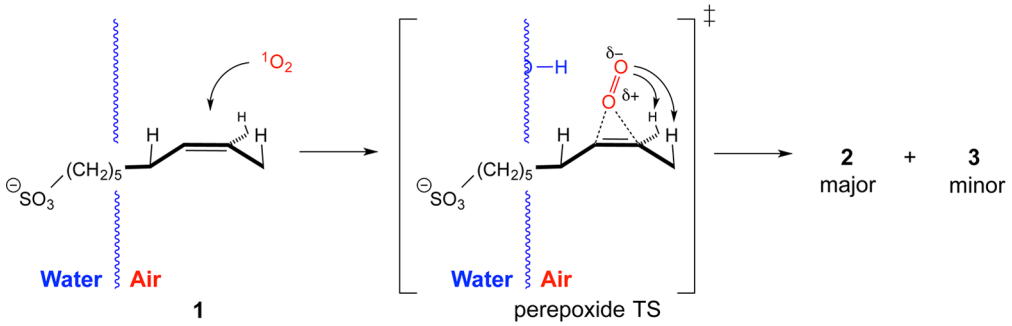

dx.doi.org/10.1021/la404564k | *Langmuir* 2014, 30, 3599−3605

Table 2. *E. coli* Inactivation by the Airborne Singlet Oxygen Treatment as a Function of Additives and Other Conditions

		E. coli inactivation				
entry	condition	*E. coli* (μg/mL)	surfactant **1** added (mM)	4:1 mixture of hydroperoxides **2** and **3** added (mM)	% killed after 1 h[b]	number of cells killed
1	airborne $^1O_2$[a]	50			25 ± 5	7.5×10^6
2		30			38 ± 5	6.8×10^6
3		15			41 ± 4	3.7×10^6
4	airborne $^1O_2$[a]	50	1.0		50 ± 6	1.5×10^7
5		30	1.0		71 ± 3	1.3×10^7
6		15	1.0		70 ± 3	6.3×10^6
7	dark	50	1.0		2.6 ± 0.5	5.2×10^4
8		30	1.0		6.3 ± 1.1	1.2×10^5
9		15	1.0		7.3 ± 2.0	1.4×10^5
10	dark	50		0.2	5 ± 1	1.0×10^5
11		30		0.2	7 ± 3	1.4×10^5
12		15		0.2	8 ± 3	1.6×10^5
13	dark	50			1.5 ± 0.5	3.0×10^3
14	669 nm light (no $^1O_2$)	50			3.7 ± 0.5	7.4×10^4
15		30			6.3 ± 0.6	1.2×10^5
16		15			8 ± 2	1.6×10^5

[a]Airborne $^1O_2$ is generated and crosses an intervening gap to the H_2O solution. [b]Error bounds were obtained from three or more measurements.

Table 3. Percent of *E. coli* Killed after Treatment with Airborne $^1O_2$ in the Presence and Absence of Hydroperoxides 2 and 3[a]

			sample additives after exposure to airborne $^1O_2$		
entry	irradiation time (min)	% *E. coli* killed by airborne $^1O_2$[b]	surfactant **1** (mM)	4:1 mixture of hydroperoxides **2** and **3** (mM)	% *E. coli* killed[b]
1	10	10 ± 2		0.01	15 ± 2[c]
2	20	16 ± 3		0.03	27 ± 3[c]
3	30	21 ± 2		0.08	30 ± 3[c]
4	45	26 ± 3		0.12	42 ± 2[c]
5	60	27 ± 5		0.15	46 ± 3[c]
6	60	28 ± 3	1.0		27 ± 4[d]

[a]Airborne $^1O_2$ is generated and crosses an intervening gap to the H_2O solution. [b]Error bounds were obtained from three measurements. [c]*E. coli* cells were treated with airborne $^1O_2$ for 1 h. Hydroperoxides **2** and **3** (in a 4:1 ratio) were added to the cells in the dark for 2 min. [d]*E. coli* cells were treated with airborne $^1O_2$ for 1 h. Surfactant **1** was then added to the cells in the dark for 2 min.

Effect of Added Hydroperoxides. The above data suggest that airborne $^1O_2$ with surfactant **1** enhanced singlet oxygen toxicity by an increase in oxidative stress (e.g., partial loss of cell membrane integrity). Evidence supporting this idea is shown in Table 3. Airborne $^1O_2$ exposure was followed with the postreaction addition of a 4:1 mixture of **2** and **3** in the dark (entries 1−5). Entries 1−5 ranged from 0.01 to 0.15 mM to mimic the hydroperoxide concentrations that form in situ for the reaction of **1** with airborne $^1O_2$ in H_2O in Figure 3.

Airborne $^1O_2$ treatment for 1 h followed by the addition of 0.15 mM hydroperoxides **2** and **3** in the dark produced a similar inactivation of 50 μg/mL *E. coli* (46%, Table 3, entry 5) compared to that of airborne $^1O_2$ with surfactant **1** (50%, Table 2, entry 4). The measured inactivation by hydroperoxides **2** and **3** was 5%, and by airborne $^1O_2$ it was 25%, whereas the amount from the combination of airborne $^1O_2$ and surfactant **1** was 50%, fully 20% greater inactivation. Pre-exposure to airborne $^1O_2$ with the postreaction addition of **1** in the dark did not enhance the *E. coli* inactivation (Table 3, entry 6). We believe that this enhanced inactivation is relevant to synergy, where $^1O_2$-predamaged cells in the presence of **2** and **3** provoke cell killing. Thus, we sought to gain insight into whether membrane damage was significant in $^1O_2$-treated cells.

We find evidence for cell permeabilization after $^1O_2$ treatment in the presence or absence of **1** based on fluorescent labeling[48] with a commercially available LIVE/DEAD *Bac*Light bacterial viability kit (Figure S17, Supporting Information). With SYTO-9 and propidium iodide stains added to 50 μg/mL *E. coli* samples after treatment and centrifugation, the propidium iodide staining of cells indicated damaged membranes. Consequently, we propose that airborne $^1O_2$ causes permeabilization but that some cells can recover. However, the presence of hydroperoxides **2** and **3** may impede such a recovery by further destabilizing the cell. In a similar vein, Redmond et al. attributes signaling and bystander effects to diffusing species such as H_2O_2 for the killing of neighboring cells adjacent to those photodynamically damaged.[49,50]

The results of this work show a heightened *E. coli* sensitivity to hydroperoxides produced in situ or added after airborne $^1O_2$ treatment. We know that $^1O_2$ exposure in the presence or absence of **1** leads to compromised cell membranes. We do not know the relative toxicities of **2** and **3**, for example, whether one hydroperoxide will cause greater membrane damage after the initial $^1O_2$ reaction. Our work also does not resolve whether **1** interacts with the cell membrane of the bacterium by adsorption or intercalation of its hydrophobic chain, but we believe that such sorption processes[51,52] play a minor role as a result of the submicellar requirement mentioned earlier for hydroperoxide **2** and **3** formation. Our interest in a relatively low 1 mM detergent **1** concentration was to potentially aim the hydrophobic group toward the surface, rather than aggregated it into a micelle away from the air/water interface. It turns out that reactive species preceding hydroperoxide formation are not likely to contribute to the toxicity because intermediates in the $^1O_2$ ene reaction are usually not thought to form.[34,53] In the absence of *E. coli*, we find no NMR evidence for facile hydroperoxide self-degradation, such as through hydroperoxide pair Russell reactions,[54] although we have not scrutinized

dx.doi.org/10.1021/la404564k | *Langmuir* 2014, 30, 3599−3605

hydroperoxide samples after 2 days when decomposition takes place.

In summary, *E. coli* oxidation was carried out with airborne $^1O_2$ and with the addition of **1** or hydroperoxides before and after $^1O_2$ exposure to examine the mechanistic aspects. A Majima–Midden-like apparatus,[9,10,12] as used here, exposes $^1O_2$ to bacteria free from the effects of sensitizer pigmentation, bleaching, and degradation. Here, the sensitizer glass plate was physically isolated from water as a means to inactivate bacteria. Offering an innovative feature, the combination of airborne $^1O_2$ with an oxidizable surfactant is promising. A ~2-fold $^1O_2$ toxicity enhancement was found in the presence of surfactant **1**.

CONCLUSIONS

The arrival of airborne $^1O_2$ to a water interface was used instead of its generation by a solvated photosensitizer. The apparatus has the advantage of being a source of gaseous singlet oxygen, otherwise the characteristics of surfactant solutions can change with added sensitizers and dyes.[55] For airborne $^1O_2$ bacterial killing, a future direction to develop may be in the presence of surfactants designed for rapid $^1O_2$ oxygenation. High $^1O_2$ oxidizability and low dark toxicity could dictate which surfactant to use. Advantages exist for reaction with tri- and tetrasubstituted alkenes. However, mono- and disubstituted alkenes are less reactive with $^1O_2$ and thus less apt to amplify $^1O_2$ toxicity. Dark toxicity is also a concern, where anionic surfactants are often less so than cationic surfactants, such as quaternary ammonium surfactants, and would be advantageous. Work on biofilms[56] coated with active $^1O_2$ ingredients or surfactants could be within reach of airborne $^1O_2$. Research efforts are in progress in this direction.

ASSOCIATED CONTENT

Supporting Information

Description of the synthesis of **1** and generation of oxidized products **2**–**5**, spectra of **1**–**5**, a cmc plot, and photographs of the apparatus. This material is available free of charge via the Internet at http://pubs.acs.org.

AUTHOR INFORMATION

Corresponding Author

*E-mail: agreer@brooklyn.cuny.edu.

Notes

The authors declare no competing financial interest.

ACKNOWLEDGMENTS

We acknowledge support from the NIH-National Institute of General Medical Sciences (NIH SC1GM093830). We thank Beth Manes for assistance in cutting the quartz vessel, Ashwini Ghogare and Mihaela Minnis for discussions, Peter Lipke for reagents, Alison Domzalski for photography work, and Leda Lee for the graphic arts work.

REFERENCES

(1) Wang, Y.; Jett, S. D.; Crum, J.; Schanze, K. S.; Chi, E. Y.; Whitten, D. G. Understanding the dark and light-enhanced bactericidal action of cationic conjugated polyelectrolytes and oligomers. *Langmuir* **2013**, *29*, 781–792.

(2) Benabbou, A. K.; Guillard, C.; Pigeot-Rémy, S.; Cantau, C.; Pigot, T.; Lejeune, P.; Derriche, Z.; Lacombe, S. Water disinfection using photosensitizers supported on silica. *J. Photochem. Photobiol., A* **2011**, *219*, 101–108.

(3) Niziolek, M.; Korytowski, W.; Girotti, A. W. Self-sensitized photodegradation of membrane-bound protoporphyrin mediated by chain lipid peroxidation: Inhibition by nitric oxide with sustained singlet oxygen damage. *Photochem. Photobiol.* **2005**, *81*, 299–305.

(4) Nardo, L.; Kristensen, S.; Tønnesen, H. H.; Høgset, A.; Lilletvedt, M. Solubilization of the photosensitizers TPCS2a and TPPS2a in aqueous media evaluated by time-resolved fluorescence analysis. *Pharmazie* **2012**, *67*, 598–600.

(5) Biasutti, M. A.; Bertolotti, S. G.; Soltermann, A. T.; García, N. A. Singlet molecular oxygen [O_2 ($^1\Delta g$)] production and quenching by hydroxybiphenyls in micellar media. *Toxicol. Environ. Chem.* **1997**, *64*, 1–13.

(6) Kruft, B. I.; Greer, A. Photosensitization reactions *in vitro* and *in vivo*. *Photochem. Photobiol.* **2011**, *87*, 1204–1213.

(7) Bolton, N. F.; Cromar, N. J.; Hallsworth, P.; Fallowfield, H. J. A review of the factors affecting sunlight inactivation of microorganism in waste stabilization ponds: preliminary results for enterococci. *Water Sci. Technol.* **2010**, *61*, 885–890.

(8) Silverman, A. I.; Peterson, B. M.; Boehm, A. B.; McNeill, K.; Nelson, K. L. Sunlight inactivation of human viruses and bacteriophages in coastal waters containing natural photosensitizers. *Environ. Sci. Technol.* **2013**, *47*, 1870–1878.

(9) Tachikawa, T.; Majima, T. Single-molecule fluorescence imaging of TiO_2 photocatalytic reactions. *Langmuir* **2009**, *25*, 7791–7802.

(10) Naito, K.; Tachikawa, T.; Cui, S.-C.; Sugimoto, A.; Fujitsuka, M.; Majima, T. Single-molecule detection of airborne singlet oxygen. *J. Am. Chem. Soc.* **2006**, *128*, 16430–16431.

(11) Eisenberg, W. C.; Taylor, K.; Murray, R. W. Gas-phase kinetics of the reaction of singlet oxygen with olefins at atmospheric pressure. *J. Phys. Chem.* **1986**, *90*, 1945–1948.

(12) Midden, W. R.; Wang, S. Y. Singlet oxygen generation for solution kinetics: clean and simple. *J. Am. Chem. Soc.* **1983**, *105*, 4129–4145.

(13) Dahl, T. A.; Midden, W. R.; Hartman, P. E. Pure singlet oxygen cytotoxic for bacteria. *Photochem. Photobiol.* **1987**, *46*, 345–352.

(14) Kautsky, H.; de Bruijn, H.; Neuwirth, R.; Baumeister, W. Energy transfers at surfaces. VII. Photosensitized oxidation mediated by a reactive, metastable state of the oxygen molecule. *Ber.* **1933**, *66B*, 1588–1600.

(15) Kautsky, H.; Hirsch, A.; Flesch, W. Energy transformations on boundary surfaces. VIII. The significance of the metastable state in photosensitized oxidations. *Ber.* **1935**, *68B*, 152–162.

(16) Rogers, S. A.; Krayer, M.; Lindsey, J. S.; Melander, C. Tandem dispersion and killing of bacteria from a biofilm. *Org. Biomol. Chem.* **2009**, *7*, 603–606.

(17) Rizvi, I.; Celli, J. P.; Evans, C. L.; Abu-Yousif, A. O.; Muzikansky, A.; Pogue, B. W.; Finkelstein, D.; Hasan, T. Synergistic enhancement of carboplatin efficacy with photodynamic therapy in a three-dimensional model for micrometastatic ovarian cancer. *Cancer Res.* **2010**, *70*, 9319–9328.

(18) Maranho, D. S.; Galvao de Lima, R.; Primo, F. L.; Santana da Silva, R.; Tedesco, A. C. Photoinduced nitric oxide and singlet oxygen release from ZnPC liposome vehicle associated with the nitrosyl ruthenium complex: synergistic effects in photodynamic therapy application. *Photochem. Photobiol.* **2009**, *85*, 705–713.

(19) St. Denis, T. G.; Vecchio, D.; Zadio, A.; Rineh, A.; Sadasivam, M.; Avci, P.; Huang, L.; Kozinska, A.; Chandran, R.; Sarna, T.; Hamblin, M. R. Thiocyanate potentiates antimicrobial photodynamic therapy: In situ generation of the sulfur trioxide radical anion by singlet oxygen. *Free Radical Biol. Med.* **2013**, *65*, 800–810.

(20) Morales, J.; Zanocco, A. L.; Günther, G.; Lemp, E. A high-performance liquid chromatography method for determination 2-(n-(*N*,*N*,*N*-trimethyl)-n-alkyl)-5-alkylfuryl halides in dipalmitoylphosphatidicholine liposome solutions. *J. Chromatogr., A* **2006**, *25*, 89–94.

(21) Albini, A.; Germani, L. Photochemical Methods. In *Handbook of Synthetic Photochemistry*; Albini, A., Fagnoni, M., Eds.; Wiley-VCH: Weinheim, Germany, 2010; pp 2–10.

(22) Jensen, R. L.; Arnbjerg, J.; Ogilby, P. R. Temperature effects on the solvent-dependent deactivation of singlet oxygen. *J. Am. Chem. Soc.* **2010**, *132*, 8098−8105.
(23) Zhao, J.; Fung, B. M. NMR study of the transformation of sodium dodecyl sulfate micelles. *Langmuir* **1993**, *9*, 1228−1231.
(24) Bartusik, D.; Minnis, M.; Ghosh, G. Autocatalytic-assisted photorelease of a sensitizer drug bound to a silica support. *J. Org. Chem.* **2013**, *78*, 8537−8544.
(25) Griesbeck, A. G.; Cho, M. 9-Mesityl-10-methylacridinium: an efficient type II and electron-transfer photooxygenation catalyst. *Org. Lett.* **2007**, *9*, 611−613.
(26) Fudickar, W.; Linker, T. Reversible photooxygenation of alkynylanthracenes: chemical generation of singlet oxygen under very mild conditions. *Chem.—Eur. J.* **2011**, *17*, 13661−13664.
(27) Geer, M. F.; Walla, M. D.; Solntsev, K. M.; Strassert, C. A.; Shimizu, L. S. Self-assembled benzophenone bis-urea macrocycles facilitate selective oxidations by singlet oxygen. *J. Org. Chem.* **2013**, *78*, 5568−5578.
(28) Wilkinson, F.; Helman, W. P.; Ross, A. B. Quantum yields for the photosensitized formation of the lowest electronically excited singlet state of molecular oxygen in solution. *J. Phys. Chem. Ref. Data* **1995**, *22*, 663−1021 especially pp 699−739.
(29) Manring, L. E.; Foote, C. S. Chemistry of singlet oxygen. 44. Mechanism of photooxidation of 2,5-dimethylhexa-2,4-diene and 2-methyl-2-pentene. *J. Am. Chem. Soc.* **1983**, *105*, 4710−4717.
(30) Dahanayake, M.; Cohen, A. W.; Rosen, M. J. Relationship of structure to properties of surfactants. 13. Surface and thermodynamic properties of some oxyethylenated sulfates and sulfonates. *J. Phys. Chem.* **1986**, *90*, 2413−2418.
(31) Zhu, Y.-P.; Masuyama, A.; Nagata, T.; Okahara, M. Preparation and surface-active properties of new amphipathic compounds with two phosphate groups and two long-chain alkyl groups. *J. Am. Oil Chem. Soc.* **1991**, *68*, 268−271.
(32) Rosen, M. J.; Kunjappu, J. T. *Surfactants and Interfacial Phenomena*, 4th ed.; Wiley: New York, 2012; pp 140−160.
(33) Stephenson, L. M.; Grdina, M. B.; Orfanopoulos, M. Mechanism of the ene reaction between singlet oxygen and olefins. *Acc. Chem. Res.* **1980**, *13*, 419−425.
(34) Singleton, D. A.; Hang, C.; Szymanski, M. J.; Meyer, M. P.; Leach, A. G.; Kuwata, K. T.; Chen, J. S.; Greer, A.; Foote, C. S.; Houk, K. N. Mechanism of ene reactions of singlet oxygen. A two-step no-intermediate mechanism. *J. Am. Chem. Soc.* **2003**, *125*, 1319−1328.
(35) Greer, A. Christopher Foote's discovery of the role of singlet oxygen [$^1O_2$ ($^1\Delta_g$)] in photosensitized oxidation reactions. *Acc. Chem. Res.* **2006**, *39*, 797−804.
(36) Ogilby, P. R.; Foote, C. S. Chemistry of singlet oxygen. 42. Effect of solvent, solvent isotopic substitution, and temperature on the lifetime of singlet molecular oxygen ($^1\Delta_g$). *J. Am. Chem. Soc.* **1983**, *105*, 3423−3430.
(37) Orfanopoulos, M.; Stratakis, M.; Elemes, Y. Geminal selectivity of singlet oxygen ene reactions. The nonbonding large group effect. *J. Am. Chem. Soc.* **1990**, *112*, 6417−6418.
(38) Clennan, E. L.; Chen, X. Geminal selectivity in singlet oxygen reactions. *J. Org. Chem.* **1988**, *53*, 3124−3126.
(39) Fristad, W. E.; Bailey, T. R.; Paquette, L. A.; Gleiter, R.; Bohm, M. C. Regiospecific photosensitized oxygenation of vinylsilanes. A method for converting saturated ketones to 1,2-transposed allylic alcohols. Possible role of silicon in directing the regioselectivity of epoxysilane cleavage reactions. *J. Am. Chem. Soc.* **1979**, *101*, 4420−4423.
(40) Tung, C.-H.; Guan, J.-Q. Remarkable product selectivity in photosensitized oxidation of alkenes within nafion membranes. *J. Am. Chem. Soc.* **1998**, *120*, 11874−11879.
(41) Robbins, R.; Ramamurthy, V. Generation and reactivity of singlet oxygen within zeolites: remarkable control of hydroperoxidation of alkenes. *Chem. Commun.* **1997**, *11*, 1071−1072.
(42) Clennan, E. L.; Sram, J. P. Photochemical reactions in the interior of a zeolite. Part 5: The origin of the zeolite induced regioselectivity in the singlet oxygen ene reaction. *Tetrahedron* **2000**, *56*, 6945−6950.
(43) Kaanumalle, L. S.; Shailaja, J.; Robbins, R. J.; Ramamurthy, V. Cation controlled singlet oxygen mediated oxidation of olefins within zeolites. *J. Photochem. Photobiol., A* **2002**, *153*, 55−65.
(44) Stratakis, M.; Raptis, C.; Sofikiti, N.; Tsangarakis, C.; Kosmas, G.; Zaravinos, I.-P.; Kalaitzakis, D.; Stavroulakis, D.; Baskakis, C.; Stathoulopoulou, A. Intrazeolite photooxygenation of chiral alkenes. Control of facial selectivity by confinement and cation−π interactions. *Tetrahedron* **2006**, *62*, 10623−10632.
(45) Houk, K. N.; Williams, P. A.; Mitchell, P. A.; Yamaguchi, K. Conformational control of reactivity and regioselectivity in singlet oxygen ene reactions: relationship to the rotational barriers of acyclic alkylethylenes. *J. Am. Chem. Soc.* **1981**, *103*, 949−950.
(46) Clennan, E. L.; Chen, X.; Koola, J. J. Steric and electronic effects on the conformations and singlet oxygen ene regiochemistries of substituted tetramethylethylenes. The origin of the geminal effect. *J. Am. Chem. Soc.* **1990**, *112*, 5193−5199.
(47) Clennan, E. L.; Cheng, X. Temperature, solvent, and substituent effects on the singlet oxidations of allylic phenyl sulfoxides, sulfones, and sulfides. *J. Am. Chem. Soc.* **1989**, *111*, 8212−8213.
(48) Boulos, L.; Prevost, M.; Barbeau, B.; Coalier, J.; Desjardins, R. LIVE/DEAD *Bac*Light: application of a new rapid staining method for direct enumeration of viable and total bacteria in drinking water. *J. Microbiol. Methods* **1999**, *37*, 77−86.
(49) Rubio, N.; Fleury, S. P.; Redmond, R. W. Spatial and temporal dynamics of in vitro photodynamic cell killing: extracellular hydrogen peroxide mediates neighbouring cell death. *Photochem. Photobiol. Sci.* **2009**, *8*, 457−464.
(50) Chakraborty, A.; Held, K. D.; Prise, K. M.; Redmond, R. W. Bystander effects induced by diffusing mediators after photodynamic stress. *Radiat. Res.* **2009**, *172*, 74−81.
(51) Rosen, M. J.; Li, F.; Morrall, S. W.; Versteeg, D. J. The relationship between the interfacial properties of surfactants and their toxicity to aquatic organisms. *Environ. Sci. Technol.* **2001**, *35*, 954−959.
(52) Zoonens, M.; Comer, J.; Masscheleyn, S.; Pebay-Peyroula, E.; Chipot, C.; Miroux, B.; Dehez, F. Dangerous liaisons between detergents and membrane proteins. The case of mitochondrial uncoupling protein 2. *J. Am. Chem. Soc.* **2013**, *135*, 15174−15182.
(53) Leach, A. G.; Houk, K. N.; Foote, C. S. Theoretical prediction of a perepoxide intermediate for the reaction of singlet oxygen with *trans*-cyclooctene contrasts with the two-step no-intermediate ene reaction for acyclic alkenes. *J. Org. Chem.* **2008**, *73*, 8511−8519.
(54) Prado, F. M.; Oliveira, M. C. B.; Miyamoto, S.; Martinez, G. R.; Medeiros, M. H. G.; Ronsein, G. E.; Di Mascio, P. Thymine hydroperoxide as a potential source of singlet molecular oxygen in DNA. *Free Radical Biol. Med.* **2009**, *47*, 401−409.
(55) Rosen, M. J.; Kunjappu, J. T. *Surfactants and Interfacial Phenomena*, 4th ed.; Wiley: New York, 2012; pp 123−125.
(56) Wang, Y.; Schanze, K. S.; Chi, E. Y.; Whitten, D. G. When worlds collide: Interactions at the interface between biological systems and synthetic cationic conjugated polyelectrolytes and oligomers. *Langmuir* **2013**, *29*, 10635−10647.